Bull. Mater. Sci., Vol. 38, No. 4, August 2015, pp. 895–899. © Indian Academy of Sciences.

Effects of crystalline growth on corrosion behaviour of nanocrystalline NiAl coating

M TAVOOSI*, H HEYDARI, A HOSSEINKHANI and B ADELIMOGHADDAM
Department of Material Engineering, Malek-Ashtar University of Technology, Shahin-Shahr, Isfahan 84156-83111, Iran

MS received 19 November 2014; accepted 16 March 2015

Abstract. **In the current work, the effect of crystalline growth on the corrosion behaviour of nanocrystalline NiAl coating was investigated. In this regard, NiAl coatings with different crystalline sizes in the range of 20–110 nm were produced by mechanical alloying, high-velocity oxy-fuel processing (HVOF) and isothermal annealing at 600°C for 0–30 h. The produced and annealed samples were characterized using X-ray diffraction, scanning electron microscopy and transmission electron microscopy. The corrosion behaviours of coatings were examined in NaCl 3/5% electrolyte by potentiostat analysis. The nanocrystalline NiAl coating with the average crystalline size of about 20 nm and the porosity content of about 2% was successfully produced by mechanical alloying and HVOF processing. By annealing the coating, the NiAl crystalline sizes increased sharply, approaching a constant value of about 110 nm. It was found that the corrosion resistance of nanocrystalline coating increased with the increase in the crystalline size.**

Keywords. **NiAl; nanostructure coating; crystalline growth; corrosion.**

1. Introduction

Nanocrystalline materials, a class of materials with crystalline size smaller than 100 nm, are synthesized by a variety of techniques such as severe plastic deformation, mechanical milling, inert gas condensation and electrodeposition processes. Interest in these materials is due to their high hardness, ductility, wear resistance and fatigue strength.[1,2] Since these materials are characterized by high volume fraction of grain boundary (as much as 10–50% of the total crystal volume),[3] their corrosion behaviour may be different from coarse grain counterparts. However, good understanding of the relation between the corrosion property and microstructure of these materials is important for both prospective engineering applications and knowledge of fundamental physicochemical properties.[4–6]

NiAl intermetallic phase is being recognized as a kind of high-temperature structural material because of excellent chemical stability, high thermal conductivity, low density and high melting point.[7,8] This compound often shows good corrosion and oxidation resistance due to the ability to form a dense, adherent and protective aluminium oxide layer.[9–11] Although many efforts have been done through formation methods and the structural, physical and mechanical properties of nanocrystalline NiAl phase,[12,13] there are few reports regarding the effect of crystalline size on the corrosion behaviour of this material. Thus, the aim of this work is to investigate the effect of crystalline size on the corrosion behaviour of nanocrystalline NiAl coating.

*Author for correspondence (ma.tavoosi@gmail.com)

2. Experimental

Starting materials were elemental aluminium (99.7% purity and particle size of 50–70 μm) and Ni (97.5% purity and particle size of 30–110 μm) powders. About 50 g of Ni and Al powder mixture, with the atomic ratio of 50 : 50, was placed in a hardened chromium steel vial of a planetary ball mill (Retsch PM100) and milled under argon atmosphere up to 90 min (ball to powder weight ratio of 10 : 1 and the rotation speed of 400 rpm). The coatings with the thickness of about 200 μm were deposited onto the grit blasted low carbon steel substrate by high-velocity oxy-fuel processing (HVOF) spraying (powder rate of 80 g min^{-1}, spray distance of 360 mm, oxygen flow rate of 830 l min^{-1}, fuel flow rate of 210 ml min^{-1} and fuel/oxygen volume ratio of 0.0253). The fuel was modified aviation turbine kerosene. Annealing of the samples was performed at 600°C for different periods of time (0–30 h) at ambient atmosphere.

X-ray diffractometer was used to study the structure of milled, deposited and annealed samples. A Philips X-PERT MPD diffractometer was used for X-ray diffraction (XRD) measurements using filtered Cu Kα radiation ($k = 0.1542$ nm). The XRD patterns were recorded in the 2θ range of 30–80° (step size of 0.03° and time per step of 1 s). The Scherrer method[14] was used to evaluate the crystallite size of NiAl phase. The microstructures of as-sprayed and annealed coatings were observed by scanning electron microscopy (SEM) in a Philips XL30 SEM at an acceleration voltage of 30 kV. Sample preparation procedure for microstructural observations was carried out by the conventional metallographic techniques. High-resolution

transmission electron microscopy (HR-TEM) in a Jeol-2010 microscope at an accelerated voltage of 200 kV was also used for microstructural investigations.

To determine the corrosion resistance of the coating, polarization corrosion testing method by a potentiostat system (EG&G Model 273A) was used. The solution and the reference electrode were NaCl 3/5% and Ag/AgCl, respectively (with the scan rate of 1 mV s^{-1}, the initial potential of −250 mV and the final potential of 250 mV).

3. Results and discussion

3.1 *Preparation of nanocrystalline NiAl coating*

Figure 1 shows the XRD patterns of $Ni_{50}Al_{50}$ powder mixture before and after 90 min of milling times. The XRD patterns of the un-milled powder mixture showed diffraction peaks of the crystalline Ni and Al phases. Increasing the milling time led to the disappearance of the Ni and Al peaks, while NiAl peaks began to appear. Complete transformation of elemental Ni and Al powder mixture to the NiAl intermetallic phase occurred after 90 min of milling. This result showed that the reaction between Al and Ni was promoted by the extensive Ni/Al interface areas as well as the short-circuit diffusion paths provided by the large number of defects such as dislocations and grain boundaries introduced during ball milling.[1] Hu *et al*[15] reported that complete transformation of Ni + Al to NiAl compound during mechanical alloying (MA) occurred after 240 h which is much longer than MA time obtained in the present study. This discrepancy can be due to the different mill machines used. The average crystalline size of the produced NiAl phase in this study was estimated about 10 nm.

The XRD pattern of the as-deposited NiAl coating is presented in figure 2. According to this figure, besides the NiAl main peaks, several additional, small, broad peaks appeared in the XRD pattern. These peaks were identified as Ni, Ni_3Al and Al_2O_3 phases. Figure 3 shows the high-magnification

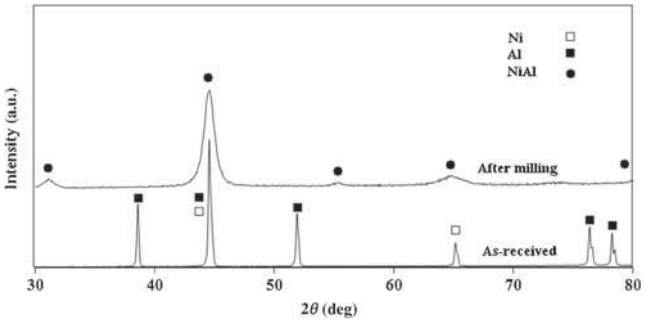

Figure 1. XRD patterns of $Ni_{50}Al_{50}$ powder mixture before and after 90 min of milling times.

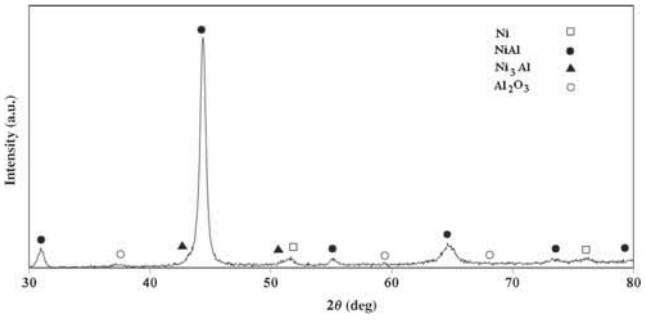

Figure 2. XRD pattern of as-deposited nanocrystalline NiAl coating.

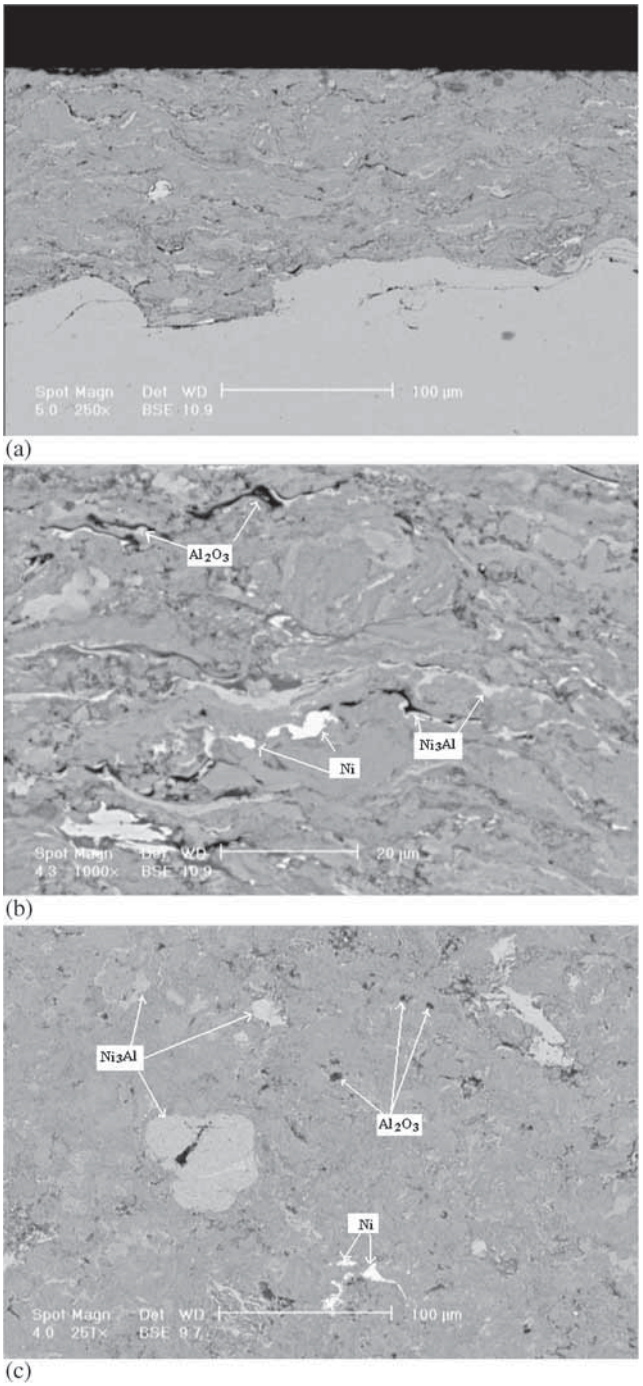

Figure 3. Cross-section (**a** and **b**) and surface (**c**) SEM micrographs of as-deposited NiAl coating.

SEM photographs of thermal sprayed coating. The coating layers generally exhibited distinct splats or lamellae as a result of impact effects during the thermal spray process. As seen, the overall coating microstructure was homogeneous and uniform with little closed pores along lamella boundaries (about 2%). According to XRD and energy-dispersive spectroscopy (EDS) analysis, these micrographs consist of four different phases: NiAl (dark grey matrix), Ni (white phase), Ni_3Al (light grey phase) and Al_2O_3 (black phase). It can be demonstrated that during HVOF processing, in some regions of NiAl phase depletion of Al atoms occurred due to oxidation, thereby the Al content reduced to the range of stability of Ni_3Al and Ni phases.[16] The crystalline size of NiAl coating was estimated via TEM (figure 4) and XRD to be about 20 nm. This confirms that NiAl coating has retained the nanocrystalline structure which is typically considered for crystalline size below 100 nm.

3.2 *Annealing the nanocrystalline coating*

In order to investigate the phase evolution during annealing, the as-deposited coating was annealed under oxidizing condition. The XRD patterns of coating after annealing at 600°C for different periods of time are shown in figure 5. As can be seen, during isothermal annealing, only narrowing of the NiAl peaks with remarkable increase in their intensities occur as a result of the increase in the crystalline sizes and decrease in the lattice strains. Figure 6 shows the SEM micrographs of annealed sample at 600°C for 30 h. As seen,

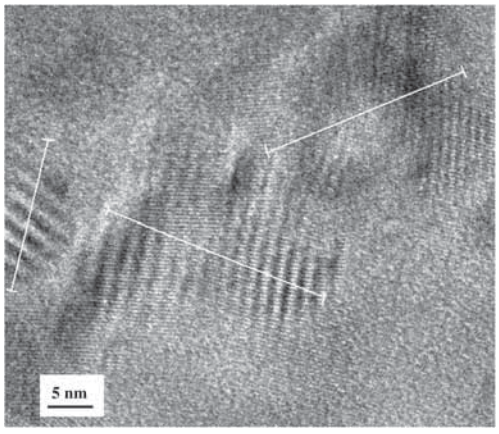

Figure 4. TEM image of as-deposited nanocrystalline NiAl coating.

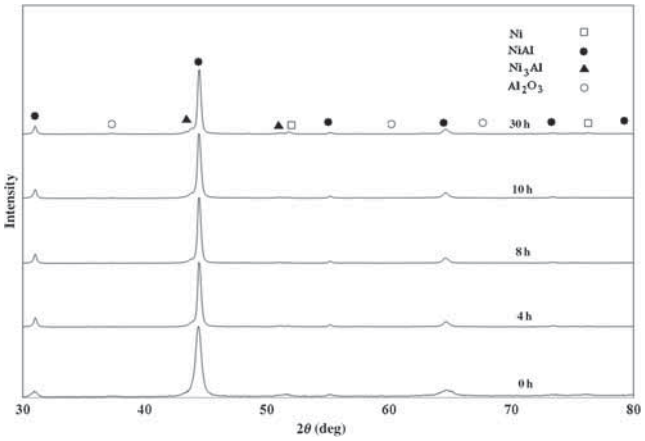

Figure 5. XRD patterns of produced NiAl coatings before and after annealing at 600°C for different periods of time.

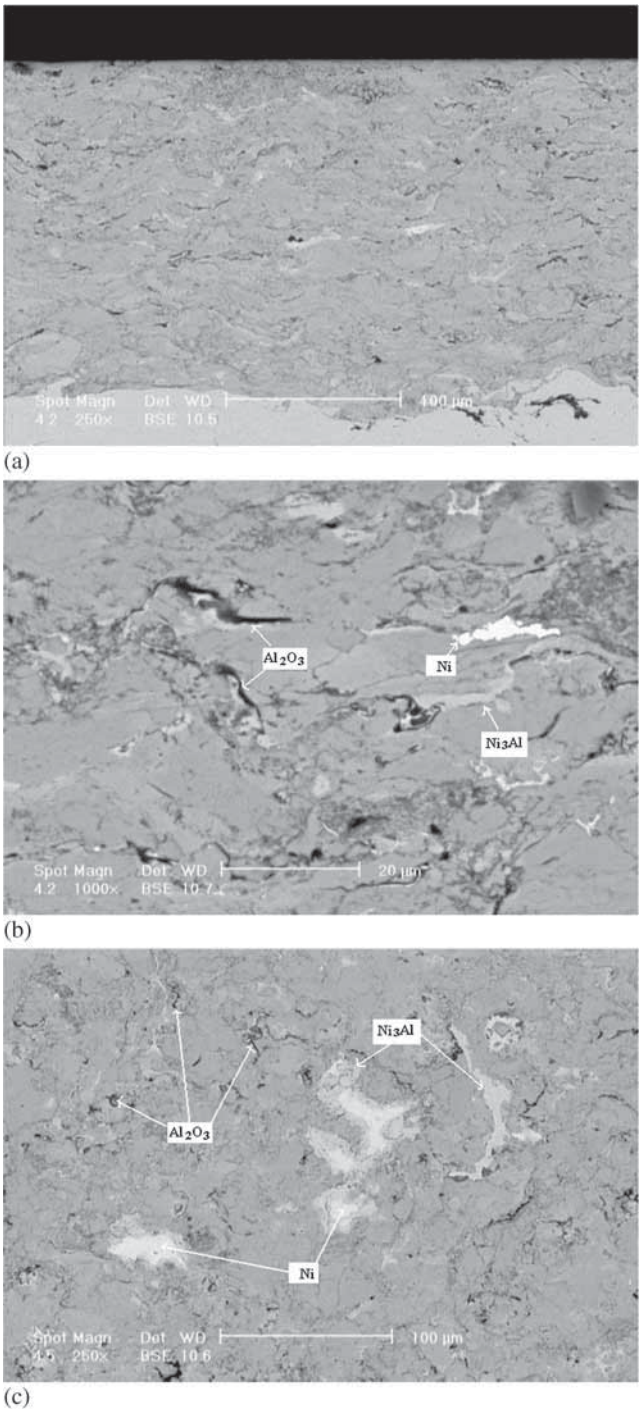

Figure 6. Cross-section (**a** and **b**) and surface (**c**) SEM micrographs of as-deposited NiAl coating after annealing at 600°C for 30 h.

there is no significant difference between these micrographs and the micrographs of coating before annealing (figure 3). Thus, during isothermal annealing in oxidation atmosphere at 600°C, gradual grain refinement was the only considerable change that occurred in the coating and no detectable reaction took place. In fact, the NiAl compound has good oxidation resistance due to the ability of this material to form a dense, adherent and protective aluminium oxide layer.[17] Moreover, the EDS analysis of annealed samples confirmed that Fe atoms could not diffuse from substrate to coating and the composition of coatings remained constant during annealing.

The crystalline sizes of the NiAl coating, determined by the Scherrer equation, as a function of annealing time is shown in figure 7a. It can be seen that substantial crystalline growth takes place at the initial annealing stage. As the annealing time is further increased up to 30 h, the crystalline growth ceases to reach an ultimate grain size of approximately 110 nm regardless of the annealing time. Figure 7b shows a typical TEM micrograph of the nanocrystalline NiAl coating annealed for 30 h. It was found that the crystalline size determined by TEM is slightly larger than that determined by XRD.

The relationship between average crystalline size and annealing time is usually expressed in the form of[18]

$$d^n - d_0^n = Kt \tag{1}$$

or

$$d - d_0 = Kt^{1/n} \tag{2}$$

where d_0 is the initial grain size, d the grain size following the annealing time t, K a constant, and n the grain growth exponent. According to equation (2), a plot of $\log(d - d_0)$ *vs.* $\log(t)$ will have a slope equal to $1/n$. By attention to figure 8, the grain growth exponent (n) for nanocrystalline NiAl coating was estimated to be about 2, which is strongly lower than the grain growth exponent ($n = 6$) in the conventional coarse-grained NiAl.[18] In fact, the presence of Ni, Ni_3Al and Al_2O_3 phases as well as porosity in microstructure, reduce the overall mobility of the boundaries in coating.[1] The above results suggest that the nanocrystalline NiAl coating exhibits crystalline size stability.

3.3 *Corrosion behaviour of coatings*

The polarization curves of NiAl nanocrystalline coating after different annealing times at 600°C are shown in figure 9. The changes of corrosion potential and corrosion current density of these samples *vs.* annealing time are also presented in figure 10. According to these figures, annealing the produced coating led to change in corrosion behaviour. The corrosion potential and current density of as-deposited coating is about −967 mV and 6.172 μA cm^{-2}, respectively. It can be observed that, by increasing the annealing time (increasing the grain size to 110 nm), the corrosion potential negatively

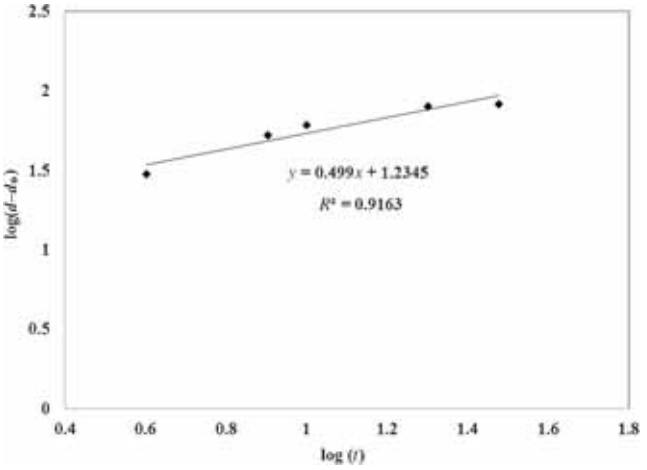

Figure 8. Plot of $\log(d - d_0)$ *vs.* $\log(t)$ for nanocrystalline NiAl coating.

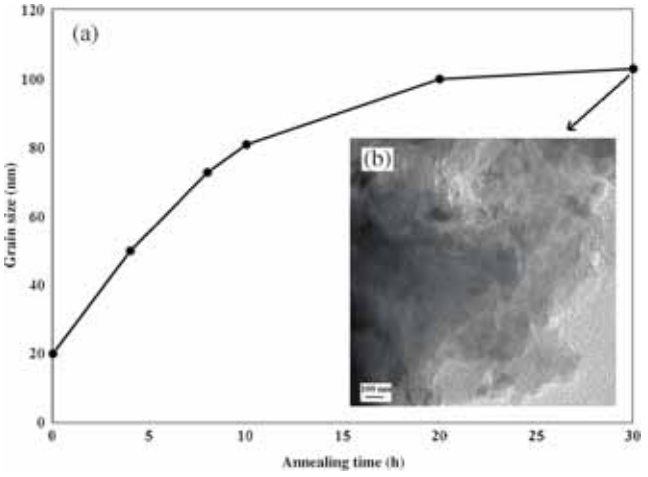

Figure 7. Average crystalline sizes of the NiAl coatings as a function of annealing time (**a**) and TEM images of as-deposited NiAl coating after annealing at 600°C for 30 h (**b**).

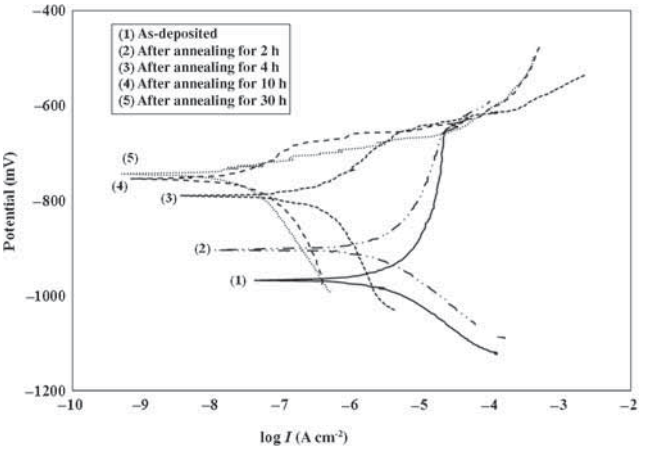

Figure 9. Polarization Tofel curves of as-deposited coating before and after annealing at 600°C for different periods of time.

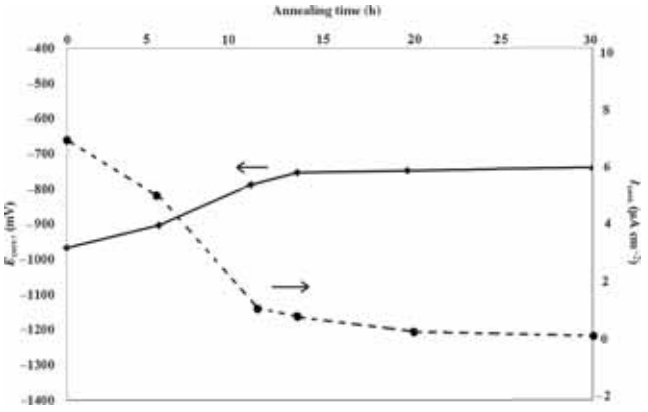

Figure 10. Corrosion potential and corrosion current density of nanocrystalline NiAl coating after annealing at 600°C for different periods of time.

shifts from −967 to −790 mV. In this condition, the corrosion current density decreases evidently from 6.172 to 0.022 μA cm^{-2}. By considering all above features, it can be concluded that the nanorystalline NiAl with the larger crystalline size should exhibit better corrosion resistance in 3.5% NaCl solution. The enhanced corrosion resistance with the increase in the crystalline sizes can be attributed to the reduction of volume fraction of grain boundaries and triple junctions as active sites for corrosion attack.[19–21]

4. Conclusions

The nanostructure NiAl intermetallic coating with the average crystalline size of about 20 nm and the porosity content of about 2% was successfully produced by MA and HVOF processing. Besides the main NiAl phase, several additional phases including Ni, Ni_3Al and Al_2O_3 were also developed in the coating due to the slight oxidation of powders during the HVOF process. By annealing the produced coating, the NiAl crystalline sizes increased sharply, approaching a constant value of about 110 nm. The corrosion resistance of NiAl coating increased with the increase in the annealing time due to the reduction of volume fraction of grain boundaries and triple junctions as active sites for corrosion attack.

References

1. Suryanarayan C 2001 *Prog. Mater. Sci.* **46** 1
2. Kumar K S, Swygenhoven H and Suresh S 2003 *Acta Mater.* **51** 5743
3. Kim H S and Bush M B 1999 *Nanostruct. Mater.* **11** 361
4. Ralston K D, Fabijanic D and Birbilis N 2011 *Electrochim. Acta* **56** 1729
5. Liu K T and Duh J G 2008 *J. Electroanal. Chem.* **618** 45
6. Argade G R, Panigrahi S K and Mishra R S 2012 *Corros. Sci.* **58** 145
7. Enayati M H, Karimzadeh F, Tavoosi M, Movahedi B and Tahvilian A 2011 *J. Therm. Spray Technol.* **20** 440
8. Stoloff N S, Liu C T and Deevi S C 2000 *Intermetallics* **8** 1313
9. Morsi K 2001 *Mater. Sci. Eng. A* **299** 1
10. Mashreghi A and Moshksar M M 2009 *J. Alloys Compd.* **482** 196
11. Deshpande S, Sampath S and Zhang H 2006 *Surf. Coat. Technol.* **200** 5395
12. Haff G R and Schulson E M 1982 *Mater. Trans. A* **13** 1563
13. Zhou L Z, Guo J T, Li G S, Xiong L Y, Wang S H and Li C G 1997 *Mater. Des.* **18** 373
14. Cullity B D 1956 *Elements of X-ray diffraction* (Addison-Wesley Publishing Company)
15. Hu W, Li M and Fukumoto M 2008 *Mater. Sci. Eng. A* **478** 1
16. Hearley J A, Little J and Sturgeon A J 2000 *Surf. Coat. Technol.* **123** 210
17. Albiter A, Espinosa-Medina M A, Gonzalez-Rodriguez J G and Perez R 2005 *Int. J. Hydrogen Energy* **30** 1311
18. Zhou L Z and Guo J T 1999 *Scr. Mater.* **40** 139
19. Wang L, Lin Y, Zeng Z, Liu W, Xue Q, Hu L and Zhang J 2007 *Electrochim. Acta* **52** 4342
20. Vinogradov A, Mimaki T and Hashimoto D S 1999 *Scr. Mater.* **41** 319
21. Fu L, Yang J, Bi Q and Liu W 2011 *Mat. Sci. Appl.* **2** 435